

A Physical Model for the Luminosity Function of High-Redshift Quasars

J. Stuart B. Wyithe¹ and Abraham Loeb

Harvard-Smithsonian Center for Astrophysics, 60 Garden St., Cambridge, MA 02138

swyithe@cfa.harvard.edu; aloeb@cfa.harvard.edu

ABSTRACT

We provide a simple theoretical model for the quasar luminosity function at high redshifts that naturally reproduces the statistical properties of the luminous SDSS quasar sample at redshifts $z \sim 4.3$ and $z \gtrsim 5.7$. Our model is based on the assumptions that quasar emission is triggered by galaxy mergers, and that the black hole mass is proportional to a power-law in the circular velocity of the host galactic halo, v_c . We assume that quasars shine at their Eddington luminosity over a time proportional to the mass ratio between the small and final galaxies in the merger. This simple model fits the quasar luminosity function at $z \sim 2-3$, reproduces the normalization and logarithmic slope ($\beta \sim -2.58$) at $z \sim 4.3$, explains the space density of bright SDSS quasars at $z \sim 6.0$, reproduces the black hole – halo mass relation for dormant black holes in the local universe, and matches the estimated duty cycle of quasar activity ($\sim 10^7$ years) in Lyman-break galaxies at $z \sim 3$. Based on the derived luminosity function we predict the resulting gravitational lensing rates for high redshift quasars. The lens fractions in the SDSS samples are predicted to be $\sim 2\%$ at $z \sim 4.3$ and $\sim 10\%$ at $z \gtrsim 5.7$. Interestingly, the limiting quasar luminosity in our best-fit relation $L \propto v_c^5/G$, scales as the binding energy of the host galaxy divided by its dynamical time, implying that feedback is the mechanism that regulates black hole growth in galactic potential wells.

Subject headings: Quasars: luminosity function - Gravitational lenses: lens statistics

1. Introduction

While the quasar luminosity function has been studied extensively at redshifts below $z \sim 3$ (e.g. Boyle, Shanks & Peterson 1988; Hartwick & Schade 1990; Pei 1995), the Sloan Digital Sky Survey (SDSS; Fukugita et al. 1996; Gunn et al. 1998; York et al. 2001) has in recent years substantially increased the number of quasars known at $z \gtrsim 3.5$ (Fan, Strauss et al. 2001a,b; Schneider et al. 2001). Two samples of very high redshift SDSS quasars have been presented to date. The first

¹Hubble Fellow

of these is a sample of 39 luminous quasars with redshifts in the range $3.6 < z < 5.0$ and a median of 4.3. The second sample consists of 4 quasars at $z \gtrsim 5.7$, including the quasar with the highest known redshift ($z = 6.28$). These samples begin to sketch out the luminosity function of quasars at $z \gtrsim 4$ and are very important for studies of the ionizing background radiation and of quasar evolution around the epoch of reionization (Haiman & Loeb 1998). Although the logarithmic slope of the luminosity function for bright quasars admits a universal value of ~ -3.5 at redshifts $z \lesssim 3$, Fan et al. (2000a) find a shallower logarithmic slope of ~ -2.5 for their luminous quasars at $z \gtrsim 3.5$. At first sight this is a puzzling result because the exponential tail of the Press-Schechter (1974) mass function describing the space density of the massive host galaxies in which bright quasars are thought to reside, becomes progressively steeper with increasing redshift.

There are several published models of varying complexity to describe the observed evolution of the quasar luminosity function within hierarchical structure formation theory (Efstathiou & Rees 1988; Small & Blandford 1992; Haehnelt & Rees 1993; Haiman & Loeb 1998; Haehnelt Natarajan & Rees 1998; Kauffmann & Haehnelt 2000). In these models, the luminosities and lifetimes of the quasars are governed by the black hole mass and the supply of cold accreting gas. The abundance and evolution of the supermassive black holes assumed to power the quasars, are linked to the evolution of the mass-function of galactic halos. The density of bright quasars is observed to decline rapidly with redshift below $z \sim 2$ (Boyle, Shanks & Peterson 1988; Hartwick & Schade 1990). This decline has been explained (Kauffman & Haehnelt 2000; see also Cavaliere & Vittorini 2000) in terms of decreases in the merger rate and the availability of cold gas to fuel the black holes. In addition, the density of bright quasars is also observed to decline beyond a redshift of $z \sim 2$ (Warren, Hewett & Osmer 1994; Schmidt, Schneider & Gunn 1995; Kennefick, Djorgovski & de Carvalho 1995). Under the assumption that quasar activity is related to the formation rate of halos, model luminosity functions have been constructed that successfully describe this decline and the shape of the luminosity function between $z \sim 2$ and $z \sim 3.5$ (Efstathiou & Rees 1988; Haehnelt & Rees 1993; Haiman & Loeb 1998; Haehnelt, Natarajan & Rees 1999; Haiman, Madau & Loeb 1999). These models predict the luminosity function at still higher redshifts. With the recent influx of results on the quasar luminosity at redshifts above $z \sim 4$, it is interesting to revisit the question of modeling the evolution of the quasar luminosity function at high redshifts. In this paper, we demonstrate that a very simple model can explain the new results on the high redshift quasar luminosity function.

Our model for the evolution of the quasar luminosity function is based on the Press-Schechter (1974) mass function and halo merger rates computed with the excursion set formalism (Bond et al. 1991; Lacy & Cole 1993). We show that this model can reproduce all of the known properties of the luminosity function above $z \sim 2$. We begin in §2 by describing an approximate version of our model (Haiman & Loeb 1998; hereafter HL98), followed by the full discussion based on the halo merger rates. In §3 and §4 we discuss the data on the quasar luminosity function and its comparison with our model. Finally we discuss the implications of our model for gravitational lensing in high-redshift samples of quasars in §5, and present our main conclusions in §6. Throughout the paper we assume

density parameters of $\Omega_m = 0.35$ in matter, $\Omega_\Lambda = 0.65$ in a cosmological constant, and a Hubble constant of $H_0 = 65 \text{ km s}^{-1} \text{ Mpc}^{-1}$. For calculations of the Press-Schechter (1974) mass function we assume a primordial power-spectrum with $n = 1$ and the fitting formula to the exact transfer function of Bardeen et al. (1986).

2. Theoretical Luminosity Functions

We compare two models for the quasar luminosity function that are based on the Press-Schechter (1974) mass function of dark matter halos, and the halo merger rates from the excursion set formalism of Bond et al. (1991) and Lacy & Cole (1993). We begin with the approximate model of HL98 which is based on the halo formation rate. We then describe our more complete model based on halo merger rates. We will demonstrate in §4.1 that only this latter model reproduces all the known features of the quasar luminosity function above $z \sim 2$, as well as the local black hole – host halo mass relation and new constraints on the quasar duty cycle.

2.1. An Approximate Model for the Quasar Luminosity Function Based on the Halo Formation Rate

HL98 discussed an approximate model for the high redshift quasar luminosity function by supposing that quasars are associated with newly formed halos. Their model assumes that each galactic halo hosts a black hole with a mass (M_{bh}) which is a constant fraction (ϵ) of the host halo mass (M_{halo}), and that the black hole shines at its Eddington rate with a universal light-curve, $f(t)$. HL98 used the derivative of the Press-Schechter mass function to approximate the formation rate of halos, arguing that mergers are rare at high redshift so that the negative contribution to the derivative is negligible. In this model the quasar luminosity as a function of time is

$$L_B(t) = M_{\text{bh}}f(t) = \epsilon M_{\text{halo}}f(t) \quad \text{for} \quad M_{\text{halo}} > M_{\text{min}}, \quad (1)$$

where $M_{\text{min}} \sim 10^8 M_\odot [(1+z)/10]^{-\frac{3}{2}}$ is the minimum halo mass inside which a black hole can form. This lower mass limit corresponds to the virial temperature below which atomic cooling is not effective in allowing the gas to sink to the center (Barkana & Loeb 2001). Following HL98 we write the resulting quasar luminosity function, defined as the comoving number density of quasars having rest frame B-band luminosities between L_B and $L_B + \Delta L_B$ and redshifts between z and $z + \Delta z$, as

$$\Psi_{\text{HL}}(L_B, z) = \int_z^\infty dz' \int_{\epsilon M_{\text{min}}}^\infty dM_{\text{bh}} \frac{d^2 n_{\text{bh}}}{dM_{\text{bh}} dz'} \delta[L_B - M_{\text{bh}}f(t_z - t')], \quad (2)$$

where t_z and t' are the time at redshifts z and z' , and $\frac{d^2 n_{\text{bh}}}{dM_{\text{bh}} dz'}$ is the change in the co-moving number density of black holes between z' and $z' + dz'$. Integrating over M_{bh} we get

$$\Psi_{\text{HL}}(L_B, z) = \int_0^{a=\frac{1}{1+z}} da \frac{dz}{da} \frac{1}{f(t_z - t)} \frac{d^2 n_{\text{bh}}}{dM_{\text{bh}} dz} \Big|_{M_{\text{bh}} = \frac{L_B}{f(t_z - t)}}, \quad (3)$$

where $a = (1 + z)^{-1}$ is the scale factor at a redshift z . HL98 used an exponential with an e -folding time $t_{\text{dc},0}$ for the universal light curve f . We find that the equivalent result for $\Psi_{\text{HL}}(L_{\text{B}}, z)$ is obtained more simply by assuming a step function for f , namely

$$f(t) = \frac{L_{\text{Edd,B}}}{M_{\text{bh}}} \Theta(t - t_{\text{dc},0}), \quad (4)$$

where $L_{\text{Edd,B}} = 5.7 \times 10^3 (M_{\text{bh}}/M_{\odot})$ is the Eddington luminosity in B-band solar luminosity units for the median quasar spectrum (Elvis et al. 1994), and $\Theta(t)$ is the Heaviside step function. We then find

$$\Psi_{\text{HL}}(L_{\text{B}}, z) = \int_{a_{\text{min}} = \frac{1}{1+z_{\text{form}}}}^{a = \frac{1}{1+z}} da \frac{dz}{da} \frac{M_{\text{bh}}}{L_{\text{Edd,B}}} \frac{d^2 n_{\text{bh}}}{dM_{\text{bh}} dz} \Big|_{M_{\text{bh}} = \frac{L_{\text{B}}}{f(tz-t)}} \quad (5)$$

given the formation redshift for the halo, z_{form} . Assuming that $t_{\text{dc},0} \ll H^{-1}(z)$, $(a - a_{\text{min}}) \approx (da/dt)t_{\text{dc},0}$, and relating the space density of black holes to the Press-Schechter (1974) mass function through

$$\frac{d^2 n_{\text{bh}}}{dM_{\text{bh}} dz} = \frac{1}{\epsilon} \frac{d^2 n_{\text{ps}}}{dM_{\text{halo}} dz}, \quad (6)$$

we obtain the following simple expression for the quasar luminosity function:

$$\Psi_{\text{HL}}(L_{\text{B}}, z) \approx \frac{t_{\text{dc},0}}{H_0^{-1}} \sqrt{\frac{\Omega_m}{a^5} + \frac{\Omega_{\Lambda}}{a^2}} \frac{1}{5.7 \times 10^3} \frac{1}{\epsilon} \frac{d^2 n_{\text{ps}}}{dM_{\text{halo}} dz} \Big|_{M_{\text{halo}} = \frac{L_{\text{B}}}{5.7 \times 10^3 \epsilon}} \quad (7)$$

We will compare this model to observations in §4.2.

2.2. A Model for the Quasar Luminosity Function Based on the Halo Merger Rate

The HL98 model associates quasar activity with halo formation. The assumption is that the halo merger rate is rarer than the halo formation rate at high redshift. However, at low redshifts the formation rate becomes smaller than the merger rate, and the derivative of the Press-Schechter mass function on which the model is based, becomes negative. Quasar activity at low redshift can be explained in relation to halo merger activity (Carlberg 1990; Kauffmann & Haehnelt 2000). In this section we discuss a simple model that associates quasar activity at high redshift with the merger rate of halos.

The merger rate of halos was computed by Lacy & Cole (1993) based on the excursion set formalism of Bond et al. (1991). We compute the number of halos having masses between ΔM_{halo} and $\Delta M_{\text{halo}} + d\Delta M_{\text{halo}}$ that accrete onto a halo of mass $M_{\text{halo}} - \Delta M_{\text{halo}}$ per unit time $\frac{d^2 N_{\text{merge}}}{d\Delta M_{\text{halo}} dt} \Big|_{M_{\text{halo}} - \Delta M_{\text{halo}}}$. Thus, the number of merger events involving the accretion of a halo of mass ΔM_{halo} by a halo of mass $M_{\text{halo}} - \Delta M_{\text{halo}}$ per unit time per comoving volume at a redshift z is given by the product

$$\frac{dn_{\text{ps}}}{dM} \Big|_{M=M_{\text{halo}} - \Delta M_{\text{halo}}} \times \frac{d^2 N_{\text{merge}}}{d\Delta M_{\text{halo}} dt} \Big|_{M_{\text{halo}} - \Delta M_{\text{halo}}}. \quad (8)$$

We assume that the mass of the central black hole scales as a power-law with the circular velocity (v_c) of the halo,

$$M_{\text{bh}} \propto v_c^\gamma. \quad (9)$$

The circular velocity of a halo of mass M_{halo} at redshift z can be written as (Barkana & Loeb 2001),

$$v_c = 159.4 \left(\frac{M_{\text{halo}}}{10^{12} h^{-1} M_\odot} \right)^{\frac{1}{3}} \left[\frac{\Omega_m}{\Omega_m^z} \frac{\Delta_c}{18\pi^2} \right]^{\frac{1}{6}} (1+z)^{\frac{1}{2}} \text{ km s}^{-1}, \quad (10)$$

where $h = (H_0/100 \text{ km s}^{-1} \text{ Mpc}^{-1})$, $\Delta_c = 18\pi^2 + 82d - 39d^2$ is the final overdensity relative to the critical density at redshift z , and $d \equiv 1 - \Omega_m^z$ with $\Omega_m^z = \frac{\Omega_m(1+z)^3}{\Omega_m(1+z)^3 + \Omega_\Lambda}$. We can therefore write,

$$\frac{M_{\text{bh}}}{M_{\text{halo}}} = \epsilon = \epsilon_o \left(\frac{M_{\text{halo}}}{10^{12} M_\odot} \right)^{\frac{\gamma}{3}-1} \left[\frac{\Omega_m}{\Omega_m^z} \frac{\Delta_c}{18\pi^2} \right]^{\frac{\gamma}{6}} h^{\gamma/3} (1+z)^{\frac{\gamma}{2}}, \quad (11)$$

and fit for two free parameters ϵ_o and γ that describe the evolution and slope of the black hole – halo mass relation. We assume that the black holes coalesce upon halo merger (Kauffmann & Haehnelt 2000) and find the number of black holes of mass between ΔM_{bh} and $\Delta M_{\text{bh}} + d\Delta M_{\text{bh}}$ that merge with black holes of mass $M_{\text{bh}} - \Delta M_{\text{bh}}$ per unit time:

$$\left. \frac{d^2 N_{\text{merge}}}{d\Delta M_{\text{bh}} dt} \right|_{M_{\text{bh}} - \Delta M_{\text{bh}}} = \frac{3}{\gamma\epsilon} \left. \frac{d^2 N_{\text{merge}}}{d\Delta M_{\text{halo}} dt} \right|_{M_{\text{halo}} - \Delta M_{\text{halo}}}. \quad (12)$$

A linear relation ($\gamma = 3$) between black hole mass and halo mass is a natural consequence of black hole growth that is dominated by coalescence with no gas accretion (Haehnelt et al. 1998). Values of $\gamma > 1$ result from significant gas accretion during the active quasar phase as deduced by Yu & Tremaine (2002). We assume that after a merger, a fraction of the cold gas from the accreted halo is driven onto the central black hole of mass M_{bh} (Mihos & Hernquist 1994; Hernquist & Mihos 1995). If the quasar shines at the Eddington rate of the black hole in the merger product (see, e.g. Yu & Tremaine 2002), then the cold gas from the small accreted halo (which makes up the new fuel reservoir) will run out in a time approximately proportional to

$$\frac{\Delta M_{\text{baryon}}}{M_{\text{halo}}} = \frac{\Delta M_{\text{halo}}}{M_{\text{halo}}} \frac{\Delta M_{\text{baryon}}}{\Delta M_{\text{halo}}}, \quad (13)$$

where ΔM_{baryon} is the mass in baryons within the accreted halo². Thus we postulate that after a merger the quasar shines at the Eddington rate corresponding to the merger product, for a time proportional to both the ratio between the masses of the accreted and initial halo and the baryon fraction of the accreted halo.

In order to examine whether the baryon mass fraction in the accreted halo would be affected by the photo-ionization heating of the intergalactic medium (IGM) after reionization, we have solved

²Equation (13) can be derived as a Taylor expansion for minor mergers. For simplicity we apply it to all mergers.

the linear growth factors D_{dm} and D_{b} for the dark matter and baryons on a spatial comoving scale $R = (3\Delta M_{\text{halo}}/4\pi\rho_{\text{m}})^{1/3}$, where ρ_{m} is the average matter density of the universe today. These growth factors obey the following set of coupled differential equations for the dark matter and baryon overdensities δ_{dm} and δ_{b} in the linear regime (e.g. Barkana & Loeb 2001):

$$\begin{aligned} \ddot{\delta}_{\text{dm}} + 2H\dot{\delta}_{\text{dm}} &= \frac{3}{2}H^2 [\Omega_{\text{b}}(z)\delta_{\text{b}} + \Omega_{\text{dm}}(z)\delta_{\text{dm}}] \\ \ddot{\delta}_{\text{b}} + 2H\dot{\delta}_{\text{b}} &= \frac{3}{2}H^2 \{[\Omega_{\text{b}}(z)\delta_{\text{b}} + \Omega_{\text{dm}}(z)\delta_{\text{dm}}]\} - \frac{k_{\text{B}}T_{\text{i}}}{\mu m_{\text{p}}} \left(\frac{k}{a}\right)^2 \left(\frac{a_{\text{i}}}{a}\right)^{1+\beta} \left[\delta_{\text{b}} + \frac{2}{3}\beta(\delta_{\text{b}} - \delta_{\text{b,i}})\right]. \end{aligned} \quad (14)$$

Here T is the gas temperature, μ the mean molecular weight (~ 0.69 for ionized IGM), k_{B} is Boltzmann's constant, and k is the co-moving wave number for the mode of interest. The subscripts i refer to quantities at an initial reference time and $\beta = 0$ or 1 for adiabatic or isothermal evolution. We assume reionization at $z_{\text{reion}} = 7$. Before reionization we assume $T_{\text{i}} = 0$; the baryon and dark-matter over-densities undergo the same evolution during this period. Following reionization, the IGM is assumed to be heated to 10^4K and to evolve isothermally ($\beta = 1$). The evolution of D_{b} is described by the superposition of solutions to equation (14) weighted by the Fourier transform of the spatial tophat window function of width R (Medvigy & Loeb 2001). Figure 1 shows the evolution of D_{b} with redshift. The curves shown correspond (from bottom to top) to halo masses of $M_{\text{halo}} = 10^6, 10^7, 10^8, 10^9, 10^{10}, 10^{11}, 10^{12}, 10^{13}$ and $10^{14}M_{\odot}$. The dark matter growth factor corresponds to the upper envelope in this figure. Prior to reionization D_{b} follows D_{dm} for all halo masses. Reionization heats the IGM and eliminates gas accretion onto small halos. The baryon overdensity in halos larger than $10^{10}M_{\odot}$ is unaffected by reionization. Thus, we find that the effect of reionization on the luminosity function is only apparent for quasars fainter than $\sim 10^{11}L_{\odot}$, which is well below the detection threshold of existing quasar surveys at $z \gg 1$, such as SDSS. We therefore assume a fixed baryon mass fraction in objects relevant for the luminosity function of bright quasars at high redshifts.

The quasar light curve and luminosity function may therefore be written as

$$f(t) = \frac{L_{\text{Edd,B}}}{M_{\text{bh}}} \Theta\left(t - \frac{\Delta M_{\text{halo}}}{M_{\text{halo}}} t_{\text{dc},0}\right), \quad (15)$$

and

$$\begin{aligned} \Psi(L_{\text{B}}, z) &= \\ \int_{\epsilon M_{\text{min}}}^{\infty} dM_{\text{bh}} \int_0^{0.5M_{\text{bh}}} d\Delta M_{\text{bh}} \int_z^{\infty} dz' \frac{dn_{\text{bh}}}{dM} \Big|_{M=M_{\text{bh}}-\Delta M_{\text{bh}}} \frac{d^2 N_{\text{merge}}}{d\Delta M_{\text{bh}} dt'} \Big|_{M_{\text{bh}}-\Delta M_{\text{bh}}} \frac{dt'}{dz'} \delta(L_{\text{B}} - M_{\text{bh}} f(t_z - t')), \end{aligned} \quad (16)$$

in analogy with equations (4) and (5), respectively. Integrating over M_{bh} we find

$$\begin{aligned} \Psi(L_{\text{B}}, z) &= \\ \int_0^{0.5M_{\text{halo}}} d\Delta M_{\text{halo}} \int_{a_{\text{min}}=\frac{1}{1+z_{\text{form}}}}^{a=\frac{1}{1+z}} da \frac{dz}{da} \frac{dn_{\text{ps}}}{dM} \Big|_{M=M_{\text{halo}}-\Delta M_{\text{halo}}} \frac{d^2 N_{\text{merge}}}{d\Delta M_{\text{halo}} dt} \Big|_{M_{\text{halo}}-\Delta M_{\text{halo}}} \frac{3}{\gamma\epsilon} \frac{dt}{dz} \frac{M_{\text{bh}}}{L_{\text{Edd,B}}}. \end{aligned} \quad (17)$$

Assuming $t_{\text{dc},0} \ll H^{-1}(z)$, we then obtain $a - a_{\text{min}} = \frac{da}{dt} t_{\text{dc},0} \frac{\Delta M_{\text{halo}}}{M_{\text{halo}}}$, yielding the luminosity function

$$\Psi(L_B, z) = \int_0^{0.5M_{\text{halo}}} d\Delta M_{\text{halo}} \frac{3}{\gamma\epsilon} \frac{t_{\text{dc},0}}{5.7 \times 10^3} \frac{\Delta M_{\text{halo}}}{M_{\text{halo}}} \frac{dn_{\text{ps}}}{dM} \Big|_{M=M_{\text{halo}}-\Delta M_{\text{halo}}} \frac{d^2 N_{\text{merge}}}{d\Delta M_{\text{halo}} dt} \Big|_{M_{\text{halo}}-\Delta M_{\text{halo}}} \quad (18)$$

where $M_{\text{halo}} = L_B/5.7 \times 10^3 \epsilon$.

The value of $t_{\text{dc},0}$ can be related to the duty cycle of quasars t_{dc} through consideration of the number of mergers during a Hubble time $H^{-1}(z)$,

$$t_{\text{dc}}(L_B, z) = t_{\text{dc},0} \int_0^{M_{\text{halo}}=\frac{0.5L_B}{5.7 \times 10^3 \epsilon}} d\Delta M_{\text{halo}} \frac{\Delta M_{\text{halo}}}{M_{\text{halo}}} H^{-1}(z) \frac{d^2 N_{\text{merge}}}{d\Delta M_{\text{halo}} dt} \Big|_{M_{\text{halo}}-\Delta M_{\text{halo}}} \quad (19)$$

We will compare the luminosity function predicted by this model with observations in §4.1.

3. The Observed Luminosity Function

The standard double power-law luminosity function (Boyle, Shanks & Peterson 1988; Pei 1995)

$$\Psi(L_B, z) = \frac{\Psi_*/L_*(z)}{[L_B/L_*(z)]^{\beta_l} + [L_B/L_*(z)]^{\beta_h}} \quad (20)$$

provides a good representation of the observed quasar luminosity function at redshifts $z \lesssim 3$. At the faint end of the luminosity function, the slope is $\beta_l = 1.51$, while at the bright end $\beta_h = 3.43$. Moreover, all dependence on redshift (at $z \lesssim 3$) is in the break luminosity L_* indicating pure luminosity evolution. At low redshift the break luminosity evolves as a power-law in redshift, and the space density of bright quasars increases with redshift. However, surveys at higher redshift show a decline in the space density of bright quasars beyond $z \sim 3$ (Warren, Hewett & Osmer 1994; Schmidt, Schneider & Gunn 1995; Kennefick, Djorgovski & de Carvalho 1995).

While quasar evolution below $z \sim 3$ is described by pure luminosity evolution, Fan et al. (2001a) found from their sample of SDSS quasars at $z \sim 4.3$ that the slope at the bright end of the luminosity function has evolved from the $z \lesssim 3$ value of $\beta_h \sim -3.5$ to $\beta_h \sim -2.5$. This result is supported by the analysis of Schmidt, Schneider & Gunn (1995). Fan et al. (2001a) also find an evolution of space density with redshift for bright quasars of $\Psi \propto 10^{-0.5z}$ between $z \sim 3.5$ and $z \sim 5$. The space density of bright quasars measured by Fan et al. (2001b) at $z \sim 6$ agrees with the extrapolation of this evolution.

We seek to model the observed features of the luminosity function at redshifts higher than the peak in quasar evolution at $z \sim 2$. In the following section we will discuss both our model (§2.2), and the HL98 model in light of the recently acquired data on quasars at high redshifts.

4. Comparison of Observed and Model Luminosity Functions

In this section we compute model luminosity functions at different redshifts and compare them with the observed quasar luminosity function. Figure 2 shows the observed luminosity function at $z = 0.1, 1.0, 2.3, 3.0, 4.0, z \sim 4.3$ and $z \sim 6.0$. Below $z \sim 4.3$, the data shown is from the summary by Pei (1995; based on the compilations of Hartwick & Schade 1990). We also show the best fit empirical luminosity function at $z \sim 4.3$ from Fan et al. (2001a) with a vertical bar to denote the quoted error in the normalization. At $z \sim 6$ the space density was inferred from Fan et al. (2001b), and the error bar includes uncertainty in the spectral index. Comparisons of this data with the halo merger rate model (§4.1) and the HL98 model (§4.2) are presented below.

4.1. The Merger Rate Model

Luminosity functions calculated from the halo merger rate model described in §2.2 are plotted as the solid lines in Figure 2 at redshifts $z = 0.1, 1.0, 2.3, 3.0, 4.0, z \sim 4.3$ and $z \sim 6.0$. In addition, the lower right panel shows predicted luminosity functions at $z = 8.0$ and $z = 10.0$. Values of $\epsilon_o = 10^{-5.2}$, $\gamma = 5$ and $t_{dc,0} = 10^{6.3}$ yr yield a good fit to the data at all $z \gtrsim 2$. The parameters in the black hole – halo mass relation bear a striking resemblance to those in the relation found by Ferrarese (2002) for the local universe, which in our notation correspond to $\epsilon_o = 10^{-5.1}$ and $\gamma = 4.71$.

The value of $t_{dc,0}$ is related to the duty cycle for different quasar luminosities and redshifts through equation (19). The duty cycle is plotted in Figure 5. For a given halo mass, t_{dc} is longer at higher redshift. Steidel et al. (2002) estimated the lifetime of bright quasar activity in a large statistical sample of Lyman-break galaxies at $z \sim 3$ to be $\sim 10^7$ yr, which is surprisingly close to our expected value of $t_{dc} = 10^{6.9}$ yr. Above $z \sim 3$ we find $t_{dc} \sim 10^7$ yr, comparable to the value inferred by comparing the local black hole density with the quasar luminosity function (e.g. Yu & Tremaine 2002). Note that while t_{dc} becomes a substantial fraction of the age of the universe at the highest redshifts considered, individual episodes of quasar activity are shorter than $t_{dc,0}$, which is an order of magnitude smaller.

Two results from the comparison between model and data stand out. First, the halo merger model reproduces the shallow slope for the $z \sim 4.3$ quasars observed by Fan et al. (2001a), and the space density of quasars at $z \sim 6.0$ measured by Fan et al. (2001b). A detailed comparison between the data and the model at $z \sim 4.3$ is shown in Figure 3. The left hand panel shows the luminosity function in the region measured by Fan et al. (2001a). The straight line with the error bar represents the empirical luminosity function (best fit slope of $\beta = -2.58$) and the uncertainty in its normalization. The upper solid line is the luminosity function of the merger rate model. The theoretical luminosity function slope is consistent with that of the observed quasars over the measured luminosity range. This is shown more clearly on the right hand panel of Figure 3 where the derivative of the model luminosity function is shown in comparison with the empirical best

fit slope (solid line) and the slope $\pm 1\sigma_\beta$ away (dashed lines). The model is consistent within the quoted uncertainty over the measured luminosity range, particularly at the fainter end. Our model luminosity function is consistent with the observed lower limit on the slope at $z = 6.0$, which Fan et al. (2000b) quote as $\beta_h < 3.9$ (95%). However the gravitational lensing rate may be very high in this sample (Wyithe & Loeb 2002a,b). While the average slope of the luminosity function cannot be changed significantly by lensing, we might easily be misled by the magnification of 1 or 2 quasars in the limited current sample of 4. Furthermore, lensing might increase the apparent space density of quasars by a factor of up to 2 (Wyithe & Loeb 2002b). The predicted luminosity functions show that the slope of the bright end becomes significantly steeper at redshifts higher than $z \sim 6$ as expected from the shape of the Press-Schechter (1974) mass function.

The fit to the luminosity function discussed above has $\gamma = 5$. An equally good fit can be obtained for $\gamma = 4$ and $\epsilon_o = 10^{-4.5}$. However this value of ϵ_o is nearly an order of magnitude larger than observed (Ferrarese 2002), and the implied duty cycle is nearly an order of magnitude too small (Yu & Tremaine 2002; Steidel et al. 2002). Hence, the complete set of observational constraints favors a value of $\gamma = 5$. Ferrarese & Merritt (2002) find a relation between M_{bh} and bulge velocity dispersion σ_b of $M_{\text{bh}} \propto \sigma_b^{4.72 \pm 0.36}$ while Tremaine et al. (2002, and references therein) find $M_{\text{bh}} \propto \sigma_b^{4.02 \pm 0.32}$. Tremaine et al. (2002) attribute this disagreement primarily to the differences in the velocity dispersion measurements used by the two groups. Unfortunately, the highly uncertain nonlinear scaling of $v_c \propto \sigma_b^{0.88 \pm 0.17}$ (Ferrarese 2002) allows the results of both groups to be consistent with our favored value of $\gamma = 5$ (which in turn translates to a mean slope of $M_{\text{bh}} \propto \sigma_b^{4.4}$, in between the slopes of the two groups).

The upper left hand panel of Figure 2 indicates that the model luminosity function provides a poorer fit to the data at redshifts $z \lesssim 2$. The density of relatively faint [$L_B \lesssim 10^{13} L_\odot$ at $z \sim 1.0$ and $L_B \lesssim 10^{12} L_\odot$ at $z \sim 0.1$ (dashed lines)] quasars is reasonably reproduced, particularly at the lowest redshift considered. The model also predicts a decline in the number of bright quasars at low redshifts. On the other hand, the slope of the model luminosity function is too shallow at the higher luminosities to explain the data. A simple observational explanation for this phenomenon might be the large drop in the average cosmic density of cold galactic gas from $z \sim 2-3$ to the present day (Storrie-Lombardi, McMahon & Irwin 1996). Furthermore, the inability of the gas to cool following the epoch of group and X-ray cluster formation would also contribute to the rapid decline in the luminosity function at low redshifts (Cavaliere & Vittorini 2000). Thus, while the merger rate predicts a decrease in the space density of quasars at low redshifts, the more complicated low redshift environments require additional modeling (e.g. Kauffmann & Haehnelt 2000) to reproduce the observed luminosity function shape.

4.2. The Halo Formation Model

We find that the HL98 model (§2.1) requires³ best-fit values of $\epsilon = 10^{-3.1}$ and $t_{\text{dc},0} = 10^{5.0}$ yr. The resulting luminosity function is shown as the dotted lines in Figures 2 and 3. The HL98 model and the halo merger model produce similar luminosity functions at $z \gtrsim 2$. However, the predicted duty cycle is too low by two orders of magnitude, and the value of ϵ produced by this fit is too high by 2 orders of magnitude to be consistent with observations.

Figures 3 and 4 indicate that the HL98 model produces a somewhat less consistent normalization at $z \sim 4.3$ and a steeper slope at $z \sim 6.0$ when compared with the halo merger model. At low redshifts the merger rate is higher than the collapse rate for halos in the mass range of interest. In fact, the derivative of the Press-Schechter (1974) mass function becomes negative and the model predicts a luminosity function with a sharp lower cutoff in luminosity (in the implementation of HL98 the smooth function, $f(t)$, results in a softer cutoff). This is seen in the upper left panel of Figure 2. If quasar activity was associated solely with the halo formation rate, then only quasars residing within the very largest halos would be observed at low redshift.

5. Rates of Multiple-Image Lensing

The fraction of quasars that are gravitationally lensed by foreground galaxies is very sensitive to the underlying luminosity function due to the potentially large magnification bias (Turner 1980; Turner, Ostriker & Gott 1984). At low redshifts ($z \lesssim 3$) the bright end of the luminosity function has a universal slope of -3.43 . However at $z \sim 4.3$ Fan et al. (2001a) observed a slope of -2.58 . Wyithe & Loeb (2002a,b) showed that empirical extrapolations of the low redshift quasar luminosity function to high redshifts yielded very different results for the gravitational lensing rate if one were to adopt a bright end slope that is -3.43 at all redshifts or a slope that is -2.58 above $z \sim 3$. Since the halo merger model described in §2.2 reproduces all measured properties of the quasar luminosity function at high redshifts, we use it to compute the magnification bias for multiple-image gravitational lenses. The magnification bias can then be used to find the fraction of all quasars (at different redshifts) that are multiply imaged. The lensing fraction for the SDSS high redshift samples was discussed at length in Wyithe & Loeb (2002a,b). We therefore give only a short summary here, and present results for the lens fraction obtained with the new luminosity function.

The probability distribution of point source magnification by a singular, spherical isothermal lens in terms of the sum of the magnifications of multiple images, μ , is $(dP/d\mu) = 8/\mu^3$ for $\mu > 2$. The bias factor for multiple imaging in a flux limited sample brighter than (absolute luminosity)

³HL98 quote $t_{\text{dc},0} = 10^{5.8}$ yr, larger than our value of $t_0 = 10^5$. Haehnelt, Natarajan & Rees (1998) also found a lower value $t_{\text{dc},0}$ in their model with constant ϵ .

$L_{\text{B,lim}}$ is therefore

$$B(z) = \frac{\int_2^\infty d\mu \frac{8}{\mu^3} \int_{L_{\text{B,lim}}/\mu}^\infty dL' \Psi(L', z)}{\int_{L_{\text{B,lim}}}^\infty dL' \Psi(L', z)}. \quad (21)$$

This magnification bias is plotted as a function of the limiting (absolute) luminosity in Figure 6. Biases at redshifts of $z = 2.3$, $z = 4.3$ and $z = 6.0$ are shown, as well as predictions for $z \sim 8.0$ and $z \sim 10.0$ (bottom to top). The bias becomes very large at high redshifts and for bright limiting magnitudes.

The resulting fraction of multiple images expected in the flux limited sample is

$$F(L_{\text{B,lim}}, z) \approx \frac{B\tau_{\text{mult}}}{B\tau_{\text{mult}} + (1 - \tau_{\text{mult}})}. \quad (22)$$

In this expression τ_{mult} is the multiple image optical depth, i.e. the source plane probability that a source will be multiply imaged for the observer. From Wyithe & Loeb (2002b) we find $\tau_{\text{mult}} = 0.0040$ for the SDSS quasars at $z \sim 4.3$ and $\tau_{\text{mult}} = 0.0059$ for the SDSS quasars at $z \sim 6$. In addition, we find $\tau_{\text{mult}} = 0.0020$, $\tau_{\text{mult}} = 0.0076$ and $\tau_{\text{mult}} = 0.0091$ (considering all galaxies as potential lenses) at $z = 2.3$, $z = 8.0$ and $z = 10.0$, respectively. The lens fraction $F(L_{\text{B,lim}}, z)$ is plotted on the right hand panel of Figure 6 for $z = 2.3, 4.3, 6.0, 8.0$ and 10.0 (bottom to top). While at low redshifts the lensing fraction is less than one percent, at higher redshifts the fraction could be much higher. The vertical dashed lines correspond to the limiting absolute luminosities of the SDSS quasar samples at $z \sim 4.3$ (left) and $z \sim 6$ (right). These limits suggest lens fractions of $\sim 2\%$ in the SDSS sample at $z \sim 4.3$ and $\sim 10\%$ in the SDSS sample at $z \gtrsim 5.7$. Note that the fractions at $z \sim 4.3$ and $z \sim 6.0$ are consistent with the value obtained for the flat luminosity function assumed in Wyithe & Loeb (2002b). At even higher redshifts the lens fraction approaches unity. The luminosity function at $z \sim 10$ predicts that quasars having luminosities brighter than a limit that corresponds to the same co-moving space density as the SDSS quasars at $z \sim 6.0$ have a lens fraction of $F \sim 0.5$.

6. Summary and Discussion

We predict the quasar luminosity function under the hypothesis that quasar activity is associated with galaxy mergers. Galactic halos are assumed to each host a black hole having a mass determined from a power-law relation with halo circular velocity, $M_{\text{bh}} \propto v_c^2$. Upon merger we assume that the gas from the accreted halo is driven to the center, and that the quasar then shines at its Eddington rate for a short period of time, proportional to the (smaller than 1/2) mass ratio between the small and final halos in the merger. Our model has 3 free parameters but at least the following 5 constraints: the luminosity function slope and normalization at $z \sim 2.5$, the evolution of the luminosity function slope and normalization, and the curvature of the luminosity function. Our model is simplified by the fact that the effect of reionization on the luminosity function is limited to luminosities much fainter than those detectable in current quasar surveys.

This very simple model reproduces all known properties of the luminosity function above $z \sim 2$, including the recently measured luminosity function slope at $z \sim 4.3$ (Fan et al. 2001a) and the space density of quasars at $z \sim 6.0$ (Fan et al. 2001b). The model suggests a black hole – halo mass relation, $M_{\text{bh}} \propto v_c^5$ consistent with that found by Ferrarese (2002) at $z = 0$, and a duty cycle of $\sim 10^7$ yr consistent with previous determinations (Yu & Tremaine 2002; Steidel et al. 2002). Using the derived luminosity function we predict the resulting lensing rates for the highest redshift samples. The recently published flux limited samples of SDSS quasars at $z \sim 4.3$ and $z \gtrsim 5.7$ are predicted to have multiple image fractions of $\sim 2\%$ and $\sim 10\%$, respectively.

The model luminosity function computed using the halo merger rates is consistent with the density of faint quasars at low redshifts, and predicts a decline in the density of bright quasars towards low redshifts, but predicts a luminosity function slope that is shallower than observed. As has been noted previously, a more careful analysis (e.g. Kauffmann & Haehnelt 2000) is required to understand the evolution of the quasar luminosity function at low redshifts. Nevertheless, the consistency of the faint quasar normalization stands in contrast to models that associate quasar activity with the halo formation rate, as those predict no faint quasars at low redshifts. Thus one is led to conclude that mergers are the likely trigger for quasar activity at all redshifts.

The $M_{\text{bh}}-v_c$ relation that provides the best fit to the data may also have a simple physical origin. First, consider dimensional analysis. If we make the minimal assumption that the limiting luminosity of a quasar is only a function of the halo circular velocity v_c , then the only dimensional parameters in the problem are v_c and G (Newton’s constant). The only combination of these parameters that has dimensions of luminosity is v_c^5/G and so we conclude

$$L_{\text{Edd}} \propto \frac{v_c^5}{G}. \quad (23)$$

What is the physics behind this relation? The value of v_c^5/G amounts to depositing the entire binding energy of a self-gravitating system during its dynamical time (so that it does not have time to adjust). The binding energy of a self-gravitating mass M is $\sim Mv_c^2$ and the dynamical time is $\sim r/v_c$. The ratio between these quantities is $\sim Mv_c^3/r$. Using the virial relation $GM/r \sim v_c^2$, we get the energy deposition rate that would unbind a self-gravitating system on its dynamical time, $\sim v_c^5/G$. A quasar may therefore unbind the gas in the galaxy around it⁴ if its power output is too large⁵ (Silk & Rees 1998; Ciotti & Ostriker 2001). As the mass of the black hole increases and the quasar’s Eddington luminosity approaches this limit, the feedback will generate a powerful galactic wind and terminate the accretion that feeds the quasar. Hence, the quasar phenomenon

⁴We implicitly assume that the central region of the galaxy (such as the proto-bulge) is characterized by a circular velocity similar to that of the galactic halo, even though it is dominated by baryons. This assumption follows naturally from the nearly flat rotation curves of nearby galaxies.

⁵Note that the power output from the quasar may include both radiation and mechanical energy. Substantial outflows are inferred to exist in broad absorption line quasars and radio galaxies [see recent summary in Furlanetto & Loeb (2002), and references therein].

may be self terminating (similarly to the formation of a proto-star). Of course, if some of the quasar energy escapes (due to incomplete absorption, partial covering factor or efficient cooling by the surrounding gas), then the feedback-limited quasar luminosity would be higher than v_c^5/G . As long as the feedback from all quasars encounters self-similar conditions in different halos, we may write

$$L_{\text{Edd}} = \beta_\epsilon \frac{v_c^5}{G}, \quad (24)$$

where β_ϵ is a constant that is related to the inferred value of ϵ_o . Equations (10), (11), (24) and the best-fit value of $\epsilon_o \sim 10^{-5.2}$ together with the relation $L_{\text{Edd}} = 1.4 \times 10^{38} (M_{\text{bh}}/M_\odot) \text{ erg s}^{-1}$, yield $\beta_\epsilon \approx 50$. We have shown that the assumption of a constant β_ϵ in equation (24) leads to a luminosity function that describes the data over a wide range of redshifts. The constancy of β_ϵ (which is also expected from dimensional analysis) implies that feedback may indeed be the mechanism that regulates the growth of supermassive black holes in galactic potential wells. The similarity between our deduced values of $\gamma = 5$ and $\epsilon_o = 10^{-5.2}$ at high redshifts and the values inferred for remnant black holes in the local universe (Ferrarese 2002; Tremaine et al. 2002), provides a strong testimony to this effect.

This work was supported in part by NSF grants AST-9900877, AST-0071019 for AL. JSBW is supported by a Hubble Fellowship grant from the Space Telescope Science Institute, which is operated by the Association of Universities for Research in Astronomy, Inc., under NASA contract NAS 5-26555.

REFERENCES

- Bardeen, J.M., Bond, J.R., Kaiser, N., & Szalay, A.S. 1986, ApJ, 304, 15
- Barkana, R., & Loeb, A. 2001, Phys. Rep., 349, 125
- Bond, J.R., Cole, S., Efstathiou, G., & Kaiser, N. 1991, ApJ, 379, 440
- Boyle, B.J., Shanks, T., & Peterson, B.A. 1988, MNRAS, 235, 935
- Carlberg, R.G. 1990, ApJ., 350, 505
- Cavaliere, A., & Vittorini, V. 2000, ApJ, 543, 599
- Ciotti, L. & Ostriker, J. P. 2001, ApJ, 551, 131
- Efstathiou, G., & Rees, M.J. 1988, MNRAS, 230, 5
- Elvis, M. et al. 1994, ApJS, 95, 1
- Fan, X., et al. 2001a AJ, 121, 54

- Fan, X., et al. 2001b AJ, 122, 2833
- Ferrarese, L. 2002, astro-ph/0203469
- Furlanetto, S. R. & Loeb, A. 2001, ApJ, 556, 619
- Haehnelt, M.G., Natarajan, P., Rees, M.J. 1998, MNRAS, 300, 817
- Haehnelt, M.G., & Rees, M.J. 1993, MNRAS, 263, 168
- Hartwick, F.D.A., & Schade, D. 1990, ARA&A, 28, 437
- Haiman, Z. & Loeb, A. 1998, ApJ, 503, 505 (HL98)
- Haiman, Z., Madau, P., & Loeb, A. 1998, ApJ, 514, 535
- Haiman, Z., & Menou, K. 2000, ApJ, 531, 42
- Hernquist, L., & Mihos, J.C. 1995, ApJ., 448, 41
- Kauffmann, G., & Haehnelt, M. 2000, MNRAS, 311, 576
- Kennefick, J.D., Djorgovski, S.G., & de Carvalho, R.R. 1995, AJ, 110, 2553
- Lacey, C., & Cole, S. 1993, MNRAS, 262, 627
- Medvigy, D., & Loeb, A. 2001, astro-ph/0110014
- Merritt, D., & Ferrarese, L., 2001, ApJ., 547, 140
- Mihos, J.C., & Hernquist, L. 1994, ApJ., 431, L9
- Pei, Y. C. 1995, ApJ, 438, 623
- Press, W. H., & Schechter, P. 1974, ApJ, 187, 425
- Schmidt, M., Schneider, D.P., & Gunn, J.E. 1995, AJ, 110, 68
- Schneider, D. P., et al. 2001, AJ, 121, 1232
- Silk, J. & Rees, M. J. 1998, A&A, 331, L1
- Small, T. A. & Blandford, R. D. 1992, MNRAS, 259, 725
- Steidel, C. et al. 2002, ApJ, in press; astro-ph/0205142
- Storrie-Lombardi, L.J., MacMahon, R.G., & Irwin, M.J. 1996, MNRAS, 283, 79
- Tremaine, S., et al., 2002, astro-ph/0203468
- Turner, E. L., Ostriker, J. P., & Gott, J. R. III 1984, ApJ, 284, 1

Turner, E. L. 1980, *ApJ*, 242, L135

Warren, S.J., Hewett, P.C., & Osmer, P.S. 1994, *ApJ.*, 421, 412

Wyithe, J. S. B., & Loeb, A. 2002, *Nature*, in press

Wyithe, J. S. B., & Loeb, A. 2002, *ApJ*, in press

Yu, Q., & Tremaine, S. 2002, *astro-ph/0203082*

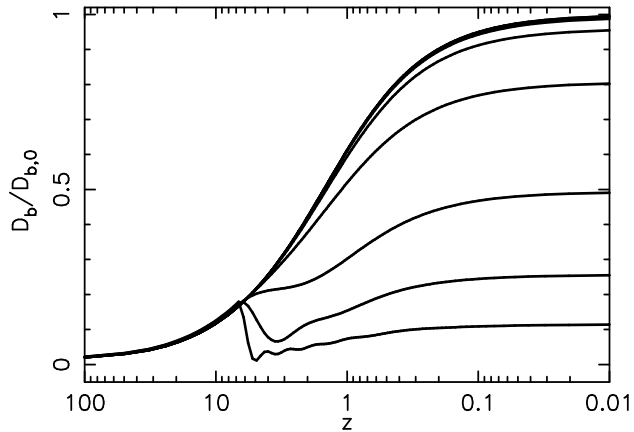


Fig. 1.— The growth factor D_b (normalized to the present day $D_{b,0}$) for baryons associated with dark matter halos of mass $M_{\text{halo}} = 10^6, 10^7, 10^8, 10^9, 10^{10}, 10^{11}, 10^{12}, 10^{13}$ and $10^{14} M_{\odot}$ (bottom to top). The down turn of the growth factor for small halos corresponds to the reionization epoch at $z_{\text{reion}} \sim 7.0$.

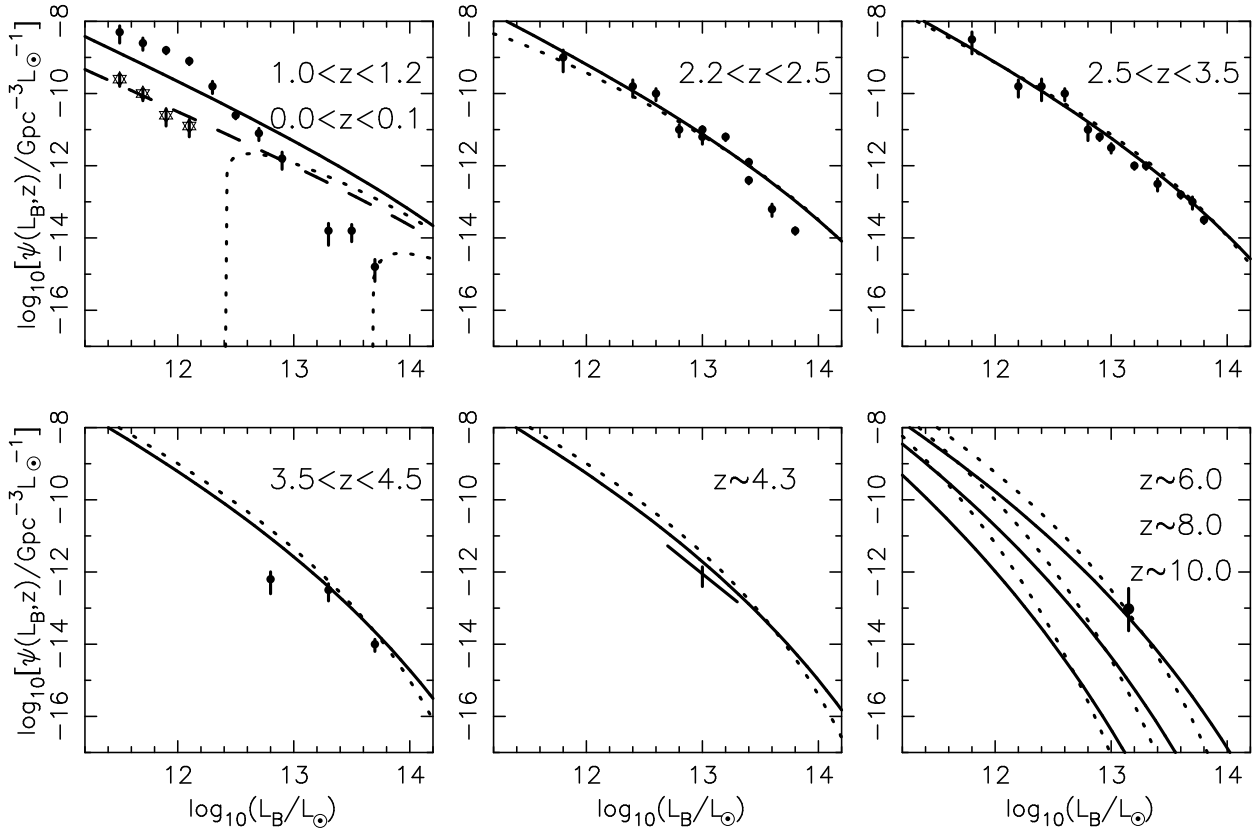


Fig. 2.— Comparison of the observed and model rest frame B-band luminosity functions. The data at $z \lesssim 4$ is summarized in Pei (1995). At $z \sim 4.3$ and $z \sim 6.0$ the data is from Fan et al. (2001a;2001b). In the $z \sim 4.3$ panel, the diagonal line shows the best fit slope of -2.58 measured by Fan et al. (2001a), and the vertical bar shows the quoted uncertainty in the normalization. In the lowest redshift panel, the dashed line and the stars represent the merger model luminosity function and the observed luminosity function data at $z \sim 0.1$ respectively. The dotted lines show the HL98 model ($\epsilon = 10^{-3.1}$, $t_{\text{dc},0} = 10^{5.0}\text{yr}$) and the solid lines are the merger model described in this paper ($\epsilon_0 = 10^{-5.2}$, $\gamma = 5$, $t_{\text{dc},0} = 10^{6.3}\text{yr}$).

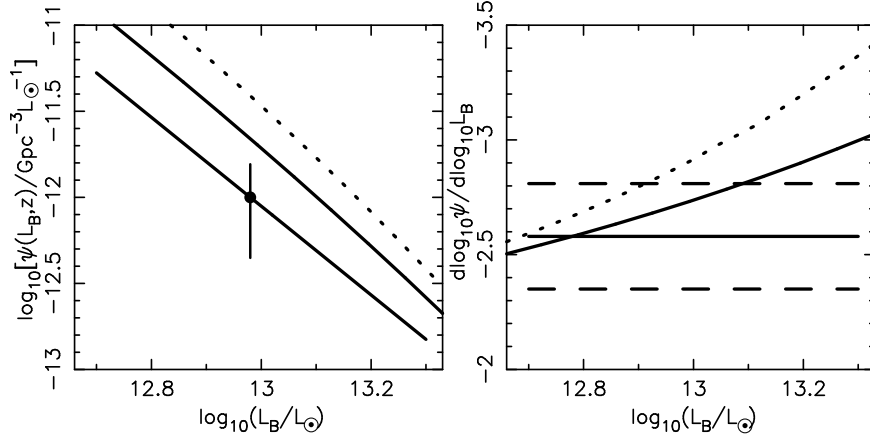


Fig. 3.— Detailed comparison of the observed rest frame B-band quasar luminosity function with the models at $z \sim 4.3$. The left panel shows the luminosity function in the region measured by Fan et al. (2001a). The straight line with the error bar shows the empirical luminosity function (best fit slope of $\beta = -2.58$) and the quoted uncertainty in the normalization. The upper solid and dotted lines show the luminosity functions for the halo merger model ($\epsilon_0 = 10^{-5.2}$, $\gamma = 5$, $t_{dc,0} = 10^{6.3}\text{yr}$) and for the HL98 model ($\epsilon = 10^{-3.1}$, $t_{dc,0} = 10^{5.0}\text{yr}$), respectively. On the right panel we show the derivatives of the model luminosity functions. The solid and dotted lines show our model and the HL98 model, respectively. The empirical best fit slope (solid) and the slopes $\pm 1\sigma_\beta = \pm 0.23$ away (dashed) are shown for comparison.

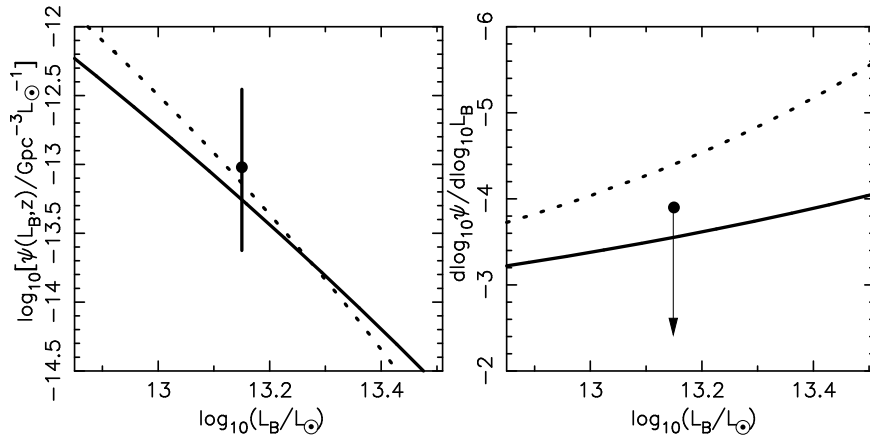


Fig. 4.— Detailed comparison of the observed rest frame B-band quasar luminosity function with the models at $z \sim 6.0$. The left panel shows the space density of quasars measured by Fan et al. (2001b). The solid and dotted lines show the luminosity functions for the halo merger model ($\epsilon_0 = 10^{-5.2}$, $\gamma = 5$, $t_{dc,0} = 10^{6.3}\text{yr}$) and for the HL98 model ($\epsilon = 10^{-3.1}$, $t_{dc,0} = 10^{5.0}\text{yr}$), respectively. On the right panel we show the derivatives of the model luminosity functions. The empirical lower limit (95%) is shown for comparison.

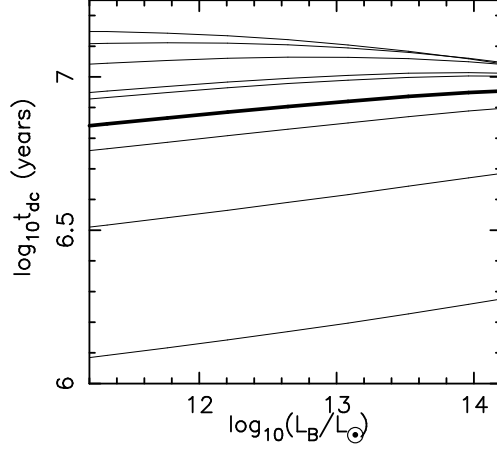


Fig. 5.— The duty cycle time t_{dc} of quasars with luminosity L_B calculated from equation (19) at redshifts $z = 0.1, 1.0, 2.3, 3.0, 4.0, 4.3, 6.0, 8.0$ and 10.0 (bottom to top, the thick line denotes the value at $z = 3.0$ which should be compared with $\sim 10^7$ yr found by Steidel et al. (2002)). The duty cycle was calculated using our best fit value of $t_{dc,0} = 10^{6.3}$ yr per merger.

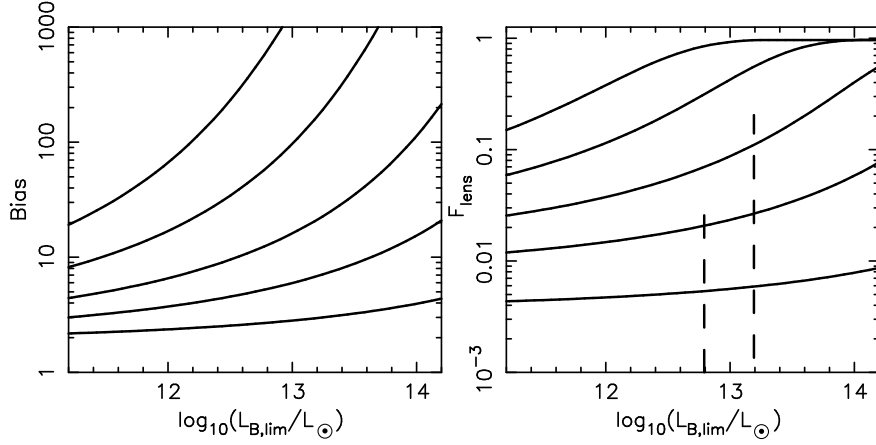


Fig. 6.— *Left:* The magnification bias as a function of absolute luminosity limit for flux limited samples of quasars at $z = 2.3, 4.3, 6.0, 8.0$ and 10.0 (bottom to top). *Right:* The multiple-image lensing rate for flux limited samples of quasars at $z = 2.3, 4.3, 6.0, 8.0$ and 10.0 (bottom to top). The left and right vertical dashed lines correspond to the absolute flux limit of the SDSS samples at $z \sim 4.3$ and $z \sim 6.0$, respectively.